Supplementary Information (SI) for Nanoscale.


# Supplementary Information: Optically induced trion formation and its control in $MoS_2$/graphene van der Waals heterostructure

Madhura Ghosh Dastidar,[†,‡,¶] Nilanjan Basu,[†,‡,¶] I-Hsuan Kao,[§] Jyoti Katoch,[§] Pramoda K. Nayak,[*,¶,†,‖] Simranjeet Singh,[§] and Vidya Praveen Bhallamudi[*,‡,†]

†*Department of Physics, Indian Institute of Technology Madras, Chennai 600036, India*

‡*Quantum Centers in Diamond and Emerging Materials (QuCenDiEM) Group, Indian Institute of Technology Madras, Chennai 600036, India*

¶*2D Materials Research and Innovation Group, Indian Institute of Technology Madras, Chennai 600036, India*

§*Department of Physics, Carnegie Mellon University, Pittsburgh, PA, 15213, USA*

‖*Centre for Nano and Material Sciences, Jain (Deemed-to-be University), Jain Global Campus, Kanakapura, Bangalore 562112, Karnataka, India*

E-mail: pramoda.nayak@jainuniversity.ac.in; praveen.bhallamudi@iitm.ac.in

## Contents

# 1 $MoS_2$ monolayer thickness

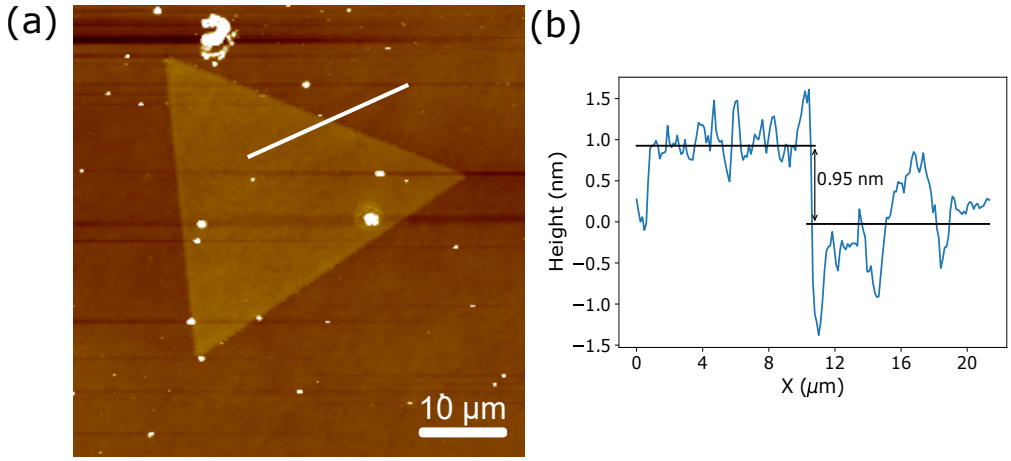


Figure S1: (a) AFM micrograph of monolayer $MoS_2$ flake used in the $MoS_2$/FLG heterostructure fabrication before transfer. (b) The height profile shows around 0.95 nm thickness, which confirms the monolayer nature of the $MoS_2$ flake.

We provide the AFM data for the $MoS_2$ flake before transfer for heterostructure fabrication [see Figs. S1 (a)-(b)]. This is done to provide the accurate thickness as upon fabrication of the heterostructure there may be an air gap between the constituent flakes increasing the errors in the AFM measurement. The AFM data shows a flake thickness of $\sim$ 0.95 nm, which proves that the flake is a monolayer.

# 2 Raman spectra for few-layer graphene

The Raman spectral measurement for FLG was performed at 300 K. We obtained the modes at 1580 $cm^{-1}$ (G peak) and 2718 $cm^{-1}$ (2D peak) [see Fig. S2]. The Raman spectrum was collected for a 60s integration time, to unravel any secondary peaks. However, the absence of a defect-activated peak and the observation of the G peak at 1580 $cm^{-1}$ indicates that a high-quality, undoped FLG flake was used for our measurements.[1] We describe the characterisation of the other components of the $MoS_2$/FLG heterostructure under "Sample structure and Raman spectra" of the main manuscript.

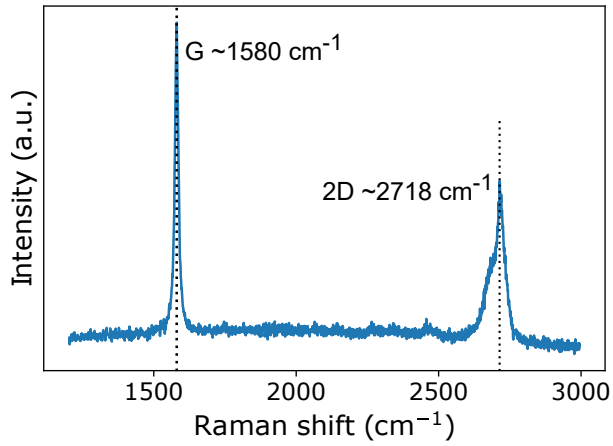


Figure S2: Raman modes measured from few-layer graphene (FLG), part of the $MoS_2$/FLG heterostructure at 300 K. The absence of a defect peak (∼1400 $cm^{-1}$) and presence of G peak at 1580 $cm^{-1}$ indicates high-quality, undoped few-layer graphene (FLG) flake.

## 3 Energy Level Scheme for Excitons and Trions

The energy level structure for trions and excitons is shown in Fig. S3. The energy of exciton recombination is higher than that of trions due to the additional energy required for binding another electron for trion formation. This is the trion binding energy ($E_b^T$).

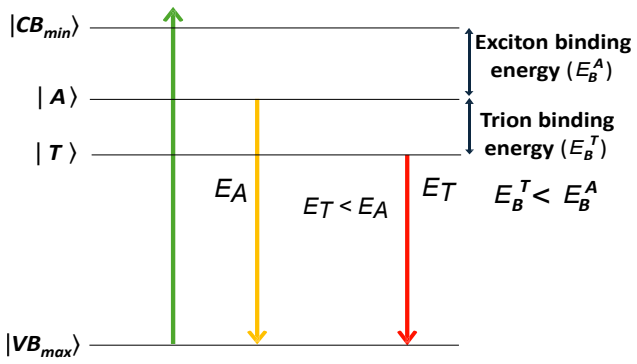


Figure S3: Schematic energy level diagram representing trion and exciton recombinations. Valence band maximum, exciton, trion and conduction band minimum states are represented by $|VB_{max}\rangle, |A\rangle, |T\rangle, |CB_{min}\rangle$, respectively. Green, orange and red arrows represent excitation, excitonic and trionic transitions, respectively. The energy of the excitonic transition ($E_A$) is greater than that of the trionic transition ($E_T$).

# 4 Discussion: Trion Peak Identification

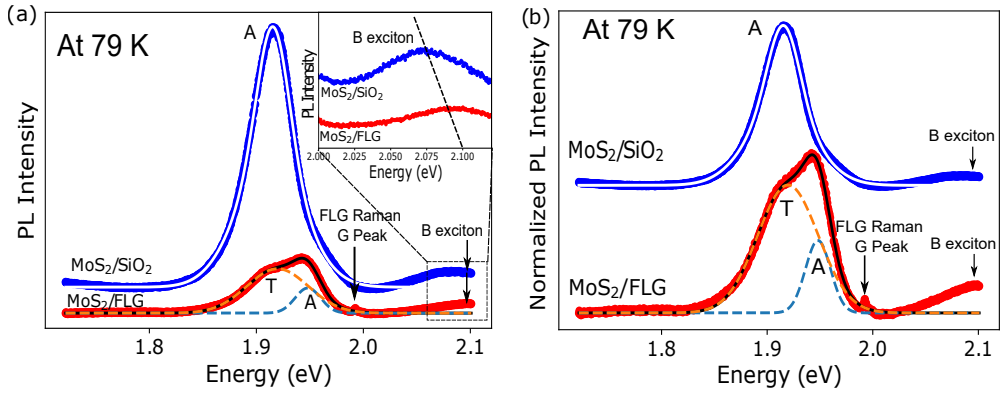


Figure S4: PL intensities $MoS_2/SiO_2$ and $MoS_2$/FLG measured at 79 K on the (a) absolute scale performed by dividing all spectra with the maximum intensity of $MoS_2/SiO_2$ at 79 K and (b) normalized scale performed by dividing both spectra with its respective maximum intensities. A manual offset is added to stack the two datasets for better visibility for each subplot. The PL peak of $MoS_2/SiO_2$ is approx. $\times 4$ higher than $MoS_2$/FLG.

A large change in the surface topology of the substrate can cause a shifted, asymmetric A excitonic peak of $MoS_2$.[2] However, this should be reflected by a shift in the in-plane Raman mode, owing to local strain [described in [2]]. In the Raman spectra we have collected, no such shift in the $E_{2g}$ peak is observed [see Fig. 1 (c) of the manuscript]. Further, a bimodal distribution from the temperature-dependent behaviour, where a selective increase of the lower energy peak is observed strongly indicates trion formation in $MoS_2$/FLG. We perform measurements across various samples and spots where the expected trends of trionic behaviour are observed. Within the confocal volume of $\sim 1\ \mu m$, identical behaviour of surface topology over different samples is highly unlikely, leading us to believe that the lower energy peak arises from trion contributions to the PL. Finally and most importantly, we obtained the power laws $\sim P^{\alpha}$, where $\alpha$ is close to 1 and $\alpha > 1$ for exciton and trion as a function of laser power density, respectively. This matches the expected trends for exciton and trion intensities as a function of incident power [described in Sec. 2.2]. If the double peak arose through PL peaks from the same quasiparticle, i.e., excitons, the power laws should reflect linear behaviour for both peaks. In Fig S4 (a)-(b) we show the PL intensities in the same

scaled and normalized by their peaks, respectively, from $MoS_2/SiO_2$ and $MoS_2$/FLG (blue and red). All the peaks are demarcated clearly. The expanded view of the B exciton in shown in the inset of Fig. S4 (a) for both $MoS_2/SiO_2$ and $MoS_2$, which behaves similarly to the A exciton, as expected.[3]

## 5 Photoluminescence: Reproducibility & Fitting Method

We present the temperature-dependent PL measurement which is crucial for evidence of trion formation and is an essential part of our analysis. Following are the sample images and measurements conducted at various spots and temperatures:

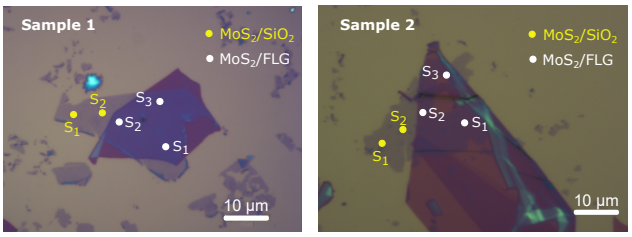


Figure S5: Optical micrographs of $MoS_2$/FLG heterostructures with the circles highlighting the various measurement spots [$S_1$: spot 1, $S_2$: spot 2, $S_3$: spot 3] on the $MoS_2$/FLG (white) and $MoS_2/SiO_2$ [$S_1$: spot 1, $S_2$: spot 2] portions.

Corresponding to the measurement spots indicated in Fig. S5, we show the temperature-dependent PL measurements conducted in the following figures.

As can be seen from Figs. S6 and S7, trion peaks are observed for $MoS_2$/FLG portion of the heterostructure as opposed to the $MoS_2/SiO_2$ portion. We have tried performing peak deconvolution with the two Gaussian functions to find if there are two peaks in the observed PL from $MoS_2/SiO_2$. However, we find the peak centers of the two Gaussians functions overlap for $MoS_2/SiO_2$ PL.

We deconvolve the primary intensity peak (A exciton) of our measured data for photoluminescence (PL) at various temperatures using the equation:

$$I(E) = A_1 e^{-(E-E_1)^2/2\sigma_{E_1}^2} + A_2 e^{-(E-E_2)^2/2\sigma_{E_2}^2} \quad (1)$$

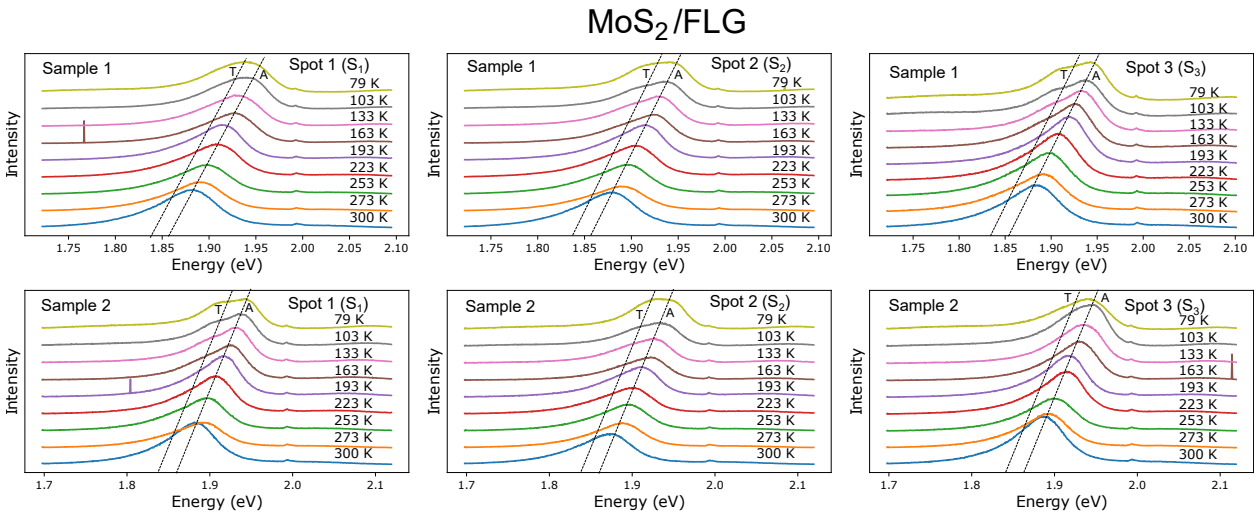


Figure S6: Temperature-dependent PL measurements for the $MoS_2$/FLG portion [top row: sample 1; bottom row: sample 2] of the heterostructure samples and measurement spots shown in Fig. S5. All plots are provided in absolute scales and a manual offset (equal for all plots) is provided to stack the PL spectra for various temperatures for better visibility. By peak deconvolution, trion and exciton peaks are extracted and peak maxima for all measured spots are joined by the line marked $T$ and $A$, respectively.

where $I(E)$ signifies the intensity as a function of photon energy, $A_1, A_2$ are the amplitudes of the two deconvolved peaks with $\sim \sigma_{E_1}, \sigma_{E_2}$ FWHM. We accounted for inhomogeneous broadening by using the fit function comprising two Gaussians. To fit the model function $I(E)$ to our measured intensity, we use `scipy.optimize.curve_fit` in Python, where we use non-linear least squares to fit a function. Thus, the data are fitted by a method of successive approximations. The advantage of this method is that it provides a complete description of the residuals associated with all the fit parameters by providing the Jacobian matrix.

Thus, we ensure a correct fitting algorithm by extracting an initial guess from the data sets' peak amplitude and FWHM. For the $MoS_2$/FLG heterostructure, the measured PL data start showing separable peak centers at temperatures below 160 K, see Fig. S8 [A, C, E]. Thus, our objective function given by Eq. 1 easily converges to the optimal parameters and describes a good fit to the measured data.

For the $MoS_2/SiO_2$ portion, we choose the initial parameters for Eq. 1 such that we

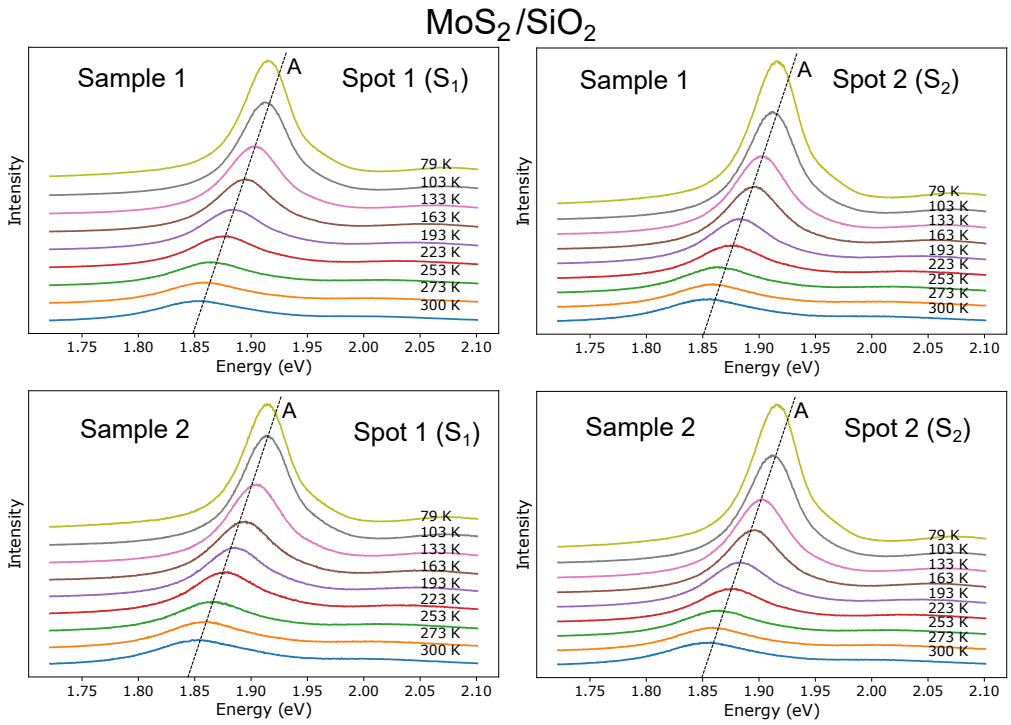


Figure S7: Temperature-dependent PL measurements for the $MoS_2/SiO_2$ portion [top row: sample 1; bottom row: sample 2] of the heterostructure samples and measurement spots shown in Fig. S5. All plots are provided in absolute scales and a manual offset (equal for all plots) is provided to stack the PL spectra for various temperatures for better visibility. By peak deconvolution, exciton peaks are extracted and peak maxima for all measured spots are joined by the line marked $A$.

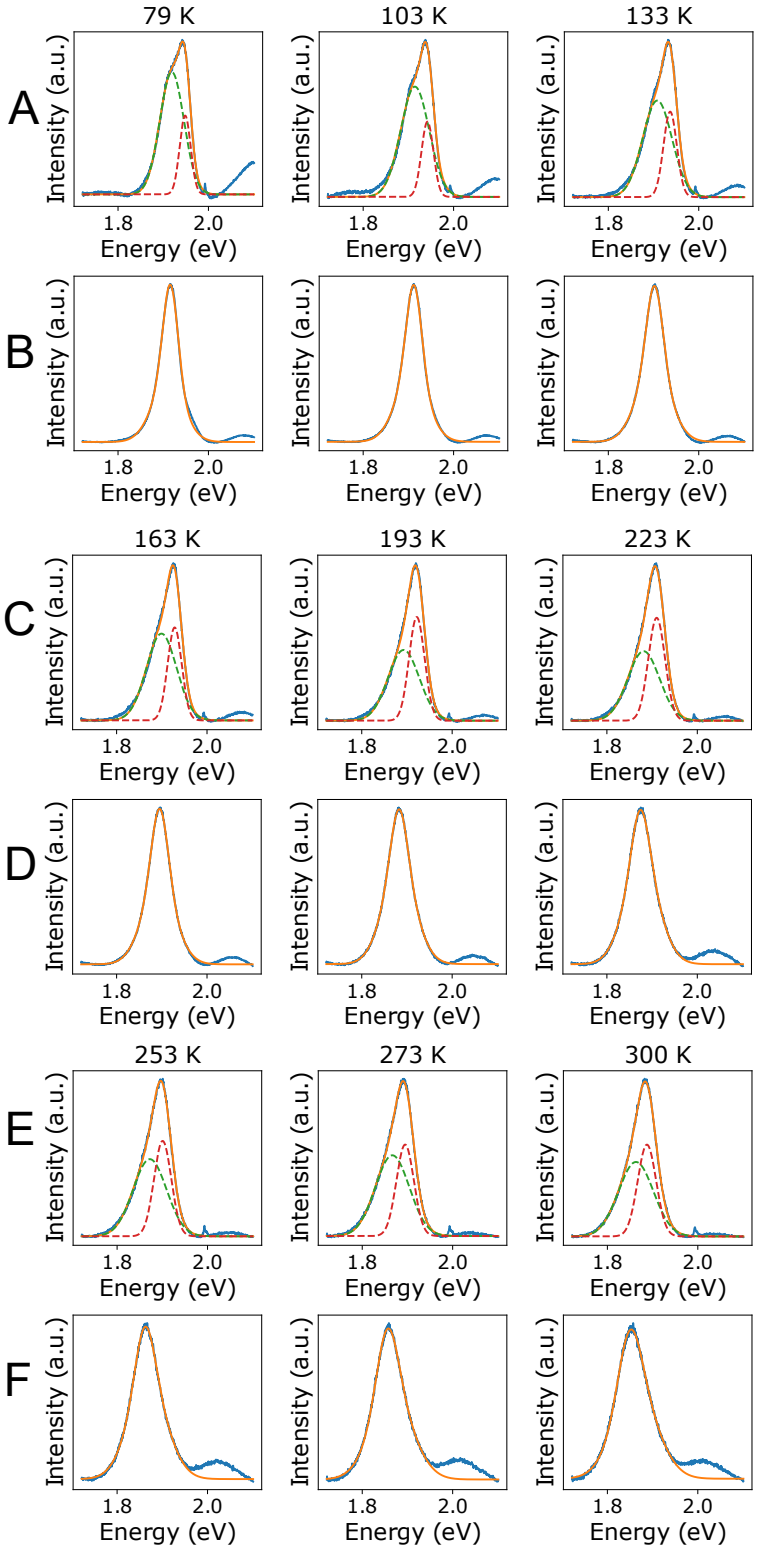


Figure S8: Temperature dependent PL spectra measured from $MoS_2$/FLG (rows A, C, E) and $MoS_2/SiO_2$ (B, D, F) heterostructure. The data depicts the increase in the concentration of trions in $MoS_2$/FLG, inversely with temperature, whereas no trions are observed in $MoS_2/SiO_2$. The fittings are performed for the A excitonic peak (which splits into 2 peaks for $MoS_2$/FLG) only.

constrain the two Gaussians to have the same peak center. However upon iteratively trying to optimize the fit, we find the function that fits better to the primary peak in the curves shown in Fig. S8 [B, D, F] is a single Gaussian:

$$I(E') = Ae^{-(E'-E)^2/2\sigma_E^2} \tag{2}$$

Thus, the observation of trions in $MoS_2$/FLG indicates the selective formation of these quasiparticles due to either excess electron doping from FLG or change in the surrounding dielectric environment. Further, we deduce that the $MoS_2/SiO_2$ portion does not show formation of trions even at temperatures below 133 K, in contrast to earlier reports.[3]

# 6 PL Spectral Characteristics

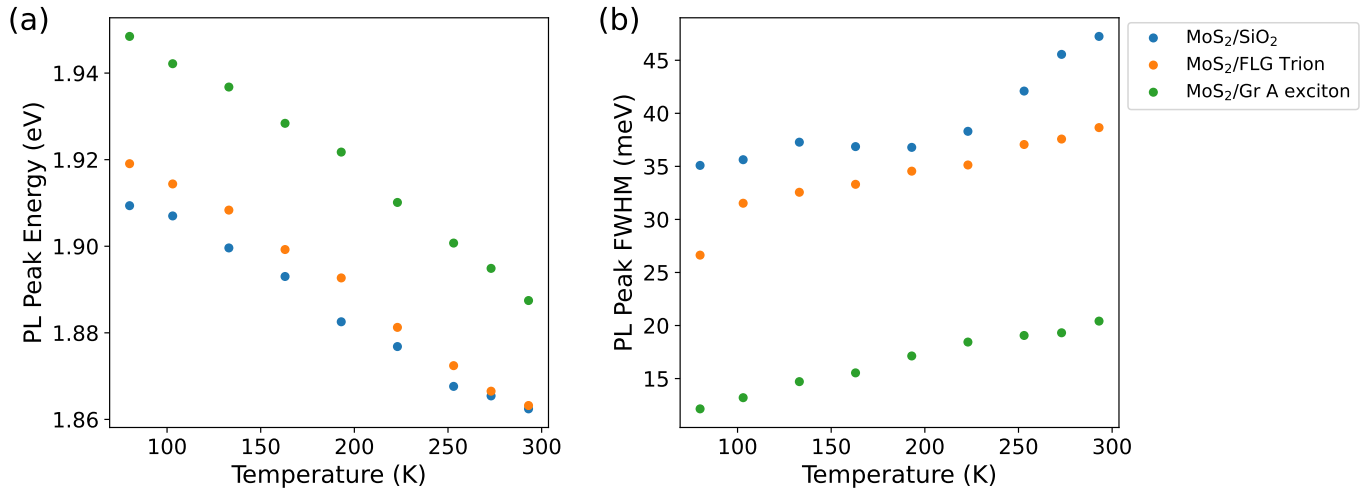


Figure S9: Variation of the A exciton (in $MoS_2/SiO_2$ and $MoS_2$/FLG) and trion (only in $MoS_2$/FLG) (a) PL peak energies and (b) FWHM as a function of temperature.

We extract the spectral properties of the PL measured from $MoS_2$/FLG and $MoS_2/SiO_2$. The PL peak energy (peak center from the fit) shown in Fig. S9 (a) for A excitons and trions in $MoS_2$/FLG and A excitons in $MoS_2/SiO_2$ as a function of temperature. We observe that all curves show a gradual red-shift with the increase in temperature. This can be attributed

to the bandgap renormalization and because the zero-momentum trion energy dominates (only for $MoS_2$/FLG) as temperature increases.[3]

In Fig. S9, the FWHM of the two peaks for $MoS_2$/FLG and the single peak of $MoS_2$/$SiO_2$ is shown. The FWHMs reduce as temperatures decrease due to the lessening of inhomogeneous broadening, as expected.

# 7 Optical control of trions

We show the control of trion densities as a function of optical excitation power in Fig. S10. At 4 different temperatures, the PL spectra is measured for $MoS_2$/FLG (top row) and $MoS_2$/$SiO_2$ (bottom row) and vertically stacked for comparison. We observe that in the bottom row corresponding to all measurements done for $MoS_2$/$SiO_2$, at low temperatures and high optical power densities, trion formation is yet not observed. Whereas, for $MoS_2$/FLG, the intensities of the doublet primary peak increase as a function of optical power. We show the extracted peak amplitudes for trions and excitons in $MoS_2$/FLG as a function of optical power density in the main manuscript Fig. 4 (a) and (b). The absence of trions in $MoS_2$/$SiO_2$ acts as a control measurement for deciphering the nature of the secondary peak in $MoS_2$/FLG, i.e., if a secondary peak would be observed for $MoS_2$/$SiO_2$, this could eradicate our argument of selective trion formation in $MoS_2$/$SiO_2$.

# 8 $MoS_2$ Raman spectra at various temperatures

Temperature-dependent Raman spectra for $MoS_2$/FLG and $MoS_2$/$SiO_2$ is shown in Fig. S11. The difference in intensity of $MoS_2$/$SiO_2$ and $MoS_2$/FLG Raman modes is due to substrate-dependent interference effects.[4] A clear observation of change in the $MoS_2$/FLG and $MoS_2$/$SiO_2$ Raman peaks is the inversion of relative intensity between the $A_{1g}$ (right peak) and $E_{2g}$ (left-peak) for $MoS_2$/FLG at 79 K. We see that the $A_{1g}$ peak (sensitive to electron doping) is greater than the $E_{2g}$ (sensitive to in-plane strain) throughout all temperatures for both por-

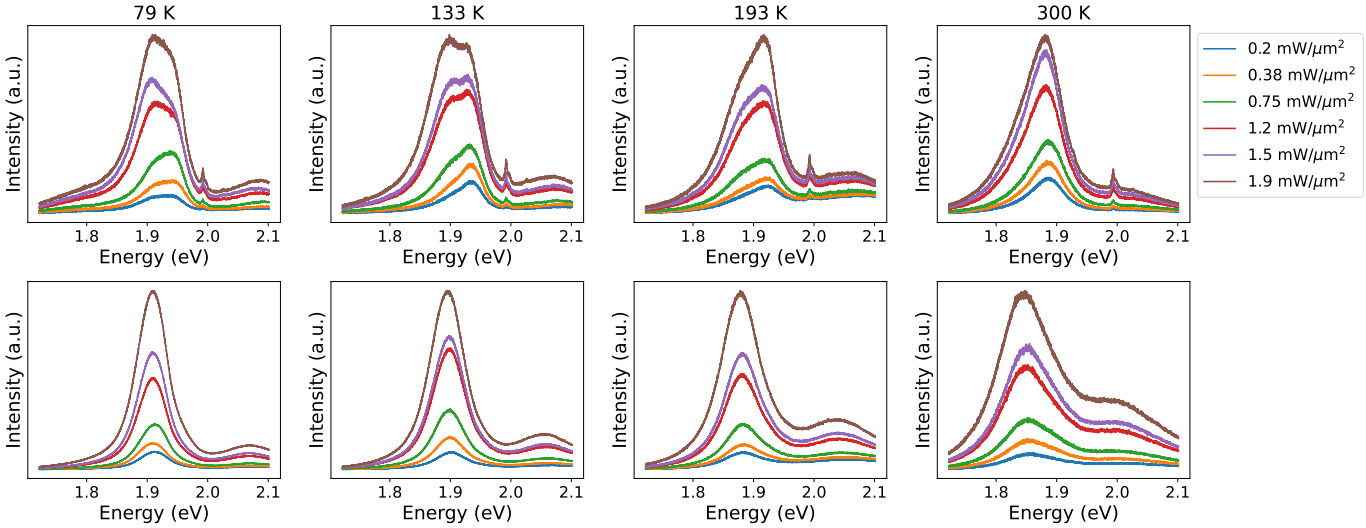


Figure S10: Excitation power dependent PL spectra measured at various temperatures for $MoS_2$/FLG (top row) and $MoS_2/SiO_2$ (bottom row). We observe that even on increasing power, trions are not formed in $MoS_2/SiO_2$.

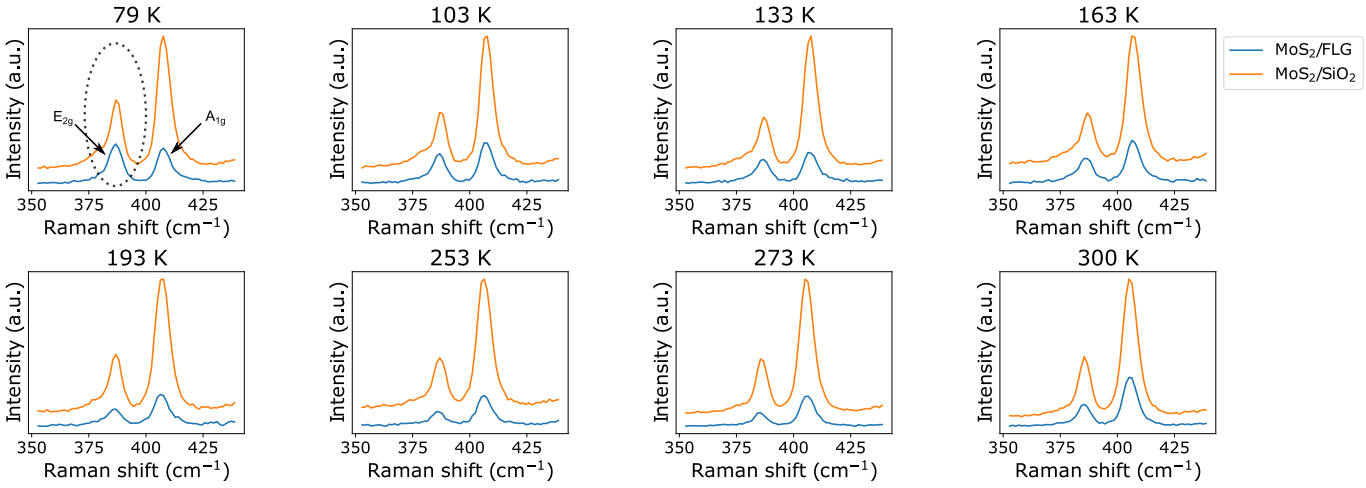


Figure S11: Temperature dependent $MoS_2$ Raman spectra measured from $MoS_2/SiO_2$ and $MoS_2$/FLG in the range 79 - 300 K. The dashed circle in the first panel indicates the increase in $E_{2g}$ mode's intensity w.r.t $A_{1g}$ for 79 K. For rest of the measured temperatures, $A_{1g}$ mode's intensity dominates that of $E_{2g}$.

tions of the heterostructure. However, at 79 K the $A_{1g}$ mode softens and shows an increased linewidth (indicated with a dashed oval in first panel of Fig. S11). This is indicative of an increase in electron doping at 79 K.[5] We plot the relative intensities of the two Raman modes as a function of temperature in Fig. 4 (d) of the main manuscript.

# 9 $MoS_2$ Raman spectra characteristics

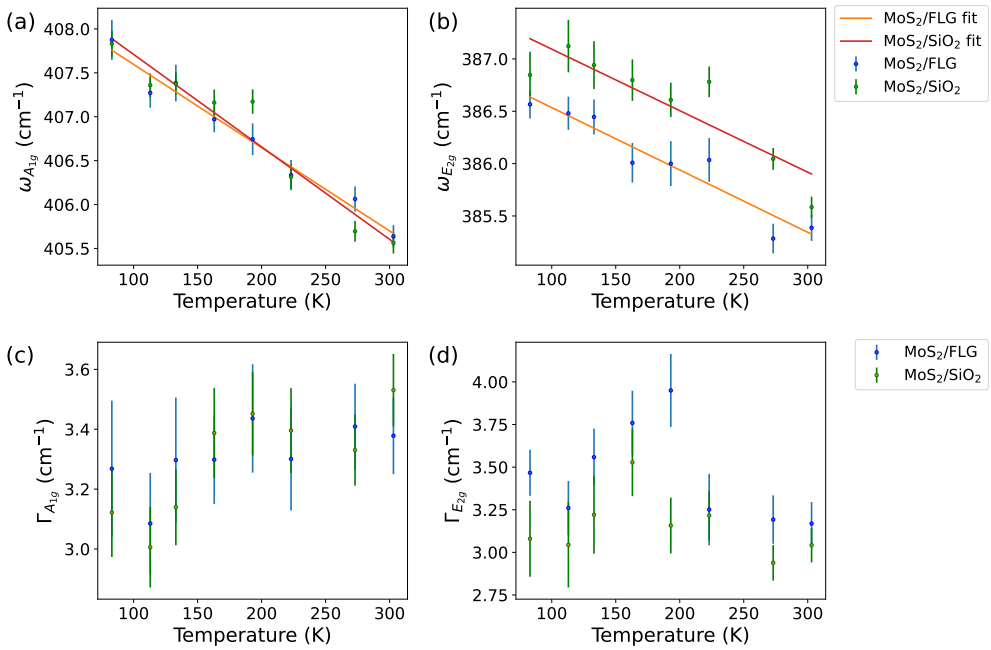


Figure S12: Extracted fit parameters from the measured $MoS_2$ Raman spectra as a function of temperature. (a), (b) shows the Raman mode frequencies of the $A_{1g}$ and $E_{2g}$ modes, respectively. (c), (d) show the linewidths of the $A_{1g}$ and $E_{2g}$ modes. While the frequencies show a linear trend which is expected for temperature-dependent Raman studies, the linewidths for each mode remain constant. This may be indicative of doping in $MoS_2$.

We fit the Raman spectra with a combination of two Lorentzian functions for the curves shown in Fig. S11 and extract the fitted parameters. Next, we plot the frequencies of the $A_{1g}$ and $E_{2g}$ Raman modes as a function of temperature, in Figs. S12 (a) and (b), respectively, for both portions of interest of the heterostructure. The frequencies are fitted to the linear function $\omega_X(T) = \omega_X(0) + A_X T$, where $\omega_X(0)$ and $A_X$ are the peak position at absolute zero temperature and the first-order temperature coefficient for $X$ ($X = A_{1g}$ or $E_{2g}$) Raman

mode. We obtain the value of $A_{A_{1g}} = -1.24 \pm 0.1 \times 10^{-2}$ cm$^{-1}$/K, which is similar to previous reports.[5]

The $E_{2g}$ mode is insensitive to any change in temperature which is expected as it is insensitive to electron doping. In Figs. S12 (c) and (d) we show the linewidths of the $A_{1g}$ and $E_{2g}$ modes as a function of temperature. While the linewidth of the $E_{2g}$ mode may remain constant due to its insensitivity to doping, the approximate constancy of $A_{1g}$ mode indicates coupling of temperature-dependent and doping effects in the properties Raman spectra.

# References


(1) Kim, S.; Park, S.; Kim, H.; Jang, G.; Park, D.; Park, J.-Y.; Lee, S.; Ahn, Y. Characterization of chemical doping of graphene by in-situ Raman spectroscopy. *Appl. Phys. Lett.* **2016**, *108*, –.

(2) Crowne, F. J.; Amani, M.; Birdwell, A. G.; Chin, M. L.; O'Regan, T. P.; Najmaei, S.; Liu, Z.; Ajayan, P. M.; Lou, J.; Dubey, M. Blueshift of the A-exciton peak in folded monolayer 1 H-MoS 2. *Physical Review B—Condensed Matter and Materials Physics* **2013**, *88*, 235302.

(3) Christopher, J. W.; Goldberg, B. B.; Swan, A. K. Long tailed trions in monolayer MoS2: Temperature dependent asymmetry and resulting red-shift of trion photoluminescence spectra. *Sci. Rep.* **2017**, *7*, 14062.

(4) Buscema, M.; Steele, G. A.; Van Der Zant, H. S.; Castellanos-Gomez, A. The effect of the substrate on the Raman and photoluminescence emission of single-layer MoS 2. *Nano Res.* **2014**, *7*, 561–571.

(5) Chakraborty, B.; Bera, A.; Muthu, D.; Bhowmick, S.; Waghmare, U. V.; Sood, A.

Symmetry-dependent phonon renormalization in monolayer MoS 2 transistor. *Phys. Rev. B* **2012**, *85*, 161403.